Aalto University

Aaltodoc
OPEN ACCESS

This is an electronic reprint of the original article.
This reprint may differ from the original in pagination and typographic detail.

Author(s): Raphaël Khan, F. Massel, and T. T. Heikkilä

Title: Tension-induced nonlinearities of flexural modes in nanomechanical resonators

Year: 2013

Version: Final published version

**Please cite the original version:**

Raphaël Khan, F. Massel, and T. T. Heikkilä. Tension-induced nonlinearities of flexural modes in nanomechanical resonators. Physical Review B, 87, 235406, June 2013. DOI: 10.1103/PhysRevB.87.235406

Rights: © 2013 Americal Physical Society (APS). Reprinted with permission.

Readers may view, browse, and/or download material for temporary copying purposes only, provided these uses are for noncommercial personal purposes. Except as provided by law, this material may not be further reproduced, distributed, transmitted, modified, adapted, performed, displayed, published, or sold in whole or part, without prior written permission from the American Physical Society.

This publication is included in the electronic version of the article dissertation:
Khan, Raphaël. Nonlinearities and quantum phenomena in nanoelectromechanical systems.
Aalto University publication series DOCTORAL DISSERTATIONS, 145/2015.

All material supplied via Aaltodoc is protected by copyright and other intellectual property rights, and duplication or sale of all or part of any of the repository collections is not permitted, except that material may be duplicated by you for your research use or educational purposes in electronic or print form. You must obtain permission for any other use. Electronic or print copies may not be offered, whether for sale or otherwise to anyone who is not an authorised user.

# Tension-induced nonlinearities of flexural modes in nanomechanical resonators

Raphaël Khan,* F. Massel, and T. T. Heikkilä
*Low Temperature Laboratory, Aalto University, P.O. Box 15100, FI-00076 AALTO, Finland*
(Received 16 November 2012; published 6 June 2013)

We consider the tension-induced nonlinearities of mechanical resonators and derive the Hamiltonian of the flexural modes up to the fourth order in the position operators. This tension can be controlled by a nearby gate voltage. We focus on systems which allow large deformations, $u(x) \gg h$, compared to the thickness $h$ of the resonator and show that in this case, the third-order coupling can become nonzero due to the induced dc deformation and offers the possibility to realize radiation-pressure-type equations of motion encountered in optomechanics. The fourth-order coupling is relevant especially for relatively low voltages. It can be detected by accessing the Duffing regime and by measuring frequency shifts due to mode-mode coupling.

DOI: 10.1103/PhysRevB.87.235406 PACS number(s): 85.85.+j, 05.45.−a

## I. INTRODUCTION

Recent progress in fabricating nanomechanical resonators has shown how these systems can be used for ultrasensitive measurements of mass, force, and charge.[1–4] Within the past few years, these systems have also entered the quantum realm,[5] as superpositions of vibrational states and zero-point vibrations have been measured. Even though such measurements can be performed in a regime where the elastic properties of the resonators could essentially be considered as linear, the extension to nonlinear conditions is well within reach of the current experimental techniques.

In this paper, we consider the generic nonlinearities of the resonators, how these show up in measurements, and how they arise when the resonators are manipulated electronically. In general, the effect of nonlinearities is twofold: on one hand, they modify in an amplitude-dependent way the resonant frequency of a given normal mode (Duffing self-nonlinearity), and on the other hand, they introduce a coupling between normal modes. Such nonlinearities show up in the presence of strong external driving, which allows one to control the coupling of different modes or detect their occupation numbers.

Motivated by the recent advances in fabricating graphene and carbon nanotube resonators,[4,6] we concentrate especially on the regime of thin resonators, where the mechanical deformation can be large compared to the resonator thickness. In this case, the major source of nonlinearity is the tension induced by the deformation itself. Starting from the mechanical energy of the deformations, we derive the generic Hamiltonian of the flexural modes, including nonlinearities up to the fourth order in the vibration amplitudes. In contrast to the results discussed in Refs. 7 and 8, where it is not taken into account, we explicitly consider the dc deformation of the resonator. This additional aspect creates an asymmetry in our system, which leads to a cubic nonlinearity. The dc deformation, dictating the strength of the nonlinearity, is driven by a nearby gate voltage, as in Fig. 1. Concentrating first on the Duffing self-nonlinearity of the modes, this then allows us to derive the voltage dependence of the Duffing constant and show that it changes sign for a certain value of voltage that depends on mode index and the amount of initial tension. This sign change results primarily from the cubic nonlinearity. Therefore, studies of the Duffing constant reveal information about the parameters of the system, in particular on the initial tension, which may otherwise be difficult to obtain by only concentrating on the voltage dependence of the mode eigenfrequencies. We go on to analyze the intermode coupling and show that the nonlinearities allow the creation of a radiation-pressure-type coupling between the different flexural modes. Such a coupling allows the realization of optomechanics-type experiments, where one of the modes is cooled or heated by driving another mode. We provide quantitative predictions for the optical spring effect (driving-induced frequency shift) and changes in effective mode damping responsible for the cooling/heating behavior and show how these can be tuned by the dc gate voltage.

## II. METHOD

The general Hamiltonian describing a nonlinear resonator is of the form

$$H = \sum_n \omega_n \hat{a}_n^\dagger \hat{a}_n + \sum_{nml} \mathbb{T}_{nml} \hat{x}_n \hat{x}_m \hat{x}_l + \sum_{nmlk} \mathbb{F}_{nmlk} \hat{x}_n \hat{x}_m \hat{x}_l \hat{x}_k + O(\hat{x}_o \hat{x}_n \hat{x}_m \hat{x}_l \hat{x}_k). \quad (1)$$

Here $\hat{x}_n = a_n^\dagger + a_n$ are the dimensionless position operators. The nonlinearities are described by the coefficients $\mathbb{T}_{nml}$ and $\mathbb{F}_{nmlk}$. The presence of $\mathbb{T}_{nml}$, like any odd nonlinearities, arises from an asymmetry in the system. In the following, we consider a mechanical resonator exhibiting the nonlinearities discussed above. We analyze a beam of mass $m$ with length $L$, thickness $h$, and cross section $S$ suspended on top of a gate capacitor at voltage $V_g$ (see Fig. 1). The flexural vibrations are characterized by the deformation $u(y,t)$ of the beam. By defining $z = y/L$, $u' = \partial_z u$ and introducing the notation $\langle u|v\rangle = \int_0^1 u(z,t)v(z,t)dz$, one can obtain (1) from the elastic energy of a resonator,[9]

$$\varepsilon[u(y,t)] = \underbrace{\frac{EI_y}{2L^3}}_{\frac{1}{2}m\omega_0^2}\langle u''|u''\rangle + \underbrace{\frac{T_0}{2L}}_{\frac{1}{2}\tau_0 m\omega_s^2}\langle u'|u'\rangle + \underbrace{\frac{ES}{8L^3}}_{\frac{1}{2h^2}m\omega_s^2}\langle u'|u'\rangle^2 + \varepsilon_{\text{force}}[u(y,t)], \quad (2)$$

 ©2013 American Physical Society

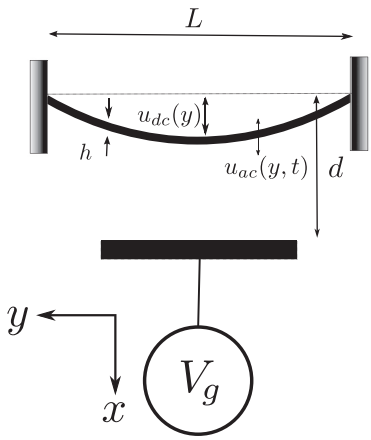


FIG. 1. Schematic picture of the studied setup: a metallic beam whose deformation is controlled by a gate voltage $V_g$ coupled to the beam via capacitance $C[d-u(y,t)]$.

with $E$ the Young modulus, $I_y$ the bending moment, $T_0$ the initial tension of the resonator, and $\varepsilon_{\rm force}$ the potential energy of the force acting on the resonator. The latter is of the form $\varepsilon_{\rm force} = -(V_g^2/2)\int_0^1 C[d-u(z,t)]dz$, where $C[d]$ is the capacitance between the gate and the beam at the distance $d$. In order to arrive at a Hamiltonian of the form given in Eq. (1), we assume that the gate voltage $V_g$ is the sum of a dc part $V_{\rm dc}$ and a small ac part $V_{\rm ac} \ll V_{\rm dc}$. These voltages lead to a static deformation $u_{\rm dc}(y) \ll d$ and a time-varying part $u_{\rm ac}(y,t) \ll u_{\rm dc}(y)$. Expanding $u_{\rm ac}(y,t)$ on an arbitrary basis $\chi_n(y)$, $u_{\rm ac} = h\sum_n x^n(t)\chi_n(y)$, we can write the potential energy containing terms with two, three, and four $y^n$'s. Writing the Hamiltonian in terms of the stress energy $E_{\rm stress} = m\omega_s^2 h^2/2 = ESh^4/(8L^3)$, these terms are characterized by the dimensionless parameters which we denote by $[\Omega^2]_m^n$, $\Lambda_{mo}^n$, and $\Theta_{mp}^{no}$ for the second-, third- and fourth-order terms, respectively. These parameters are described in detail in the Appendix. In particular, they depend on the dc bias voltage $V_{\rm dc}$ and the total tension $T$ in the beam. As discussed below, the latter also depends on $V_{\rm dc}$. The behavior of the coefficient $[\Omega^2]_m^n$ determines the voltage dependence of the eigenfrequency, as described in Refs. 10 and 11. For $V_{\rm dc} = 0$, third-order terms $\Lambda_{mo}^n$ vanish because of symmetry ($u_{\rm dc} = 0$), but for large $V_{\rm dc}$, they grow as $\Lambda_{mo}^n \propto V_g^{2/3}$. The voltage dependence of the fourth-order terms $\Theta_{mp}^{no}$, on the other hand, is weak and in our analytical approximations (see Appendix) is disregarded altogether.

We arrive at the desired form (1) by writing the Hamiltonian in a basis which diagonalizes $[\Omega^2]_m^n$ and scaling the amplitude $hx_n$ of each mode by its zero-point motion $x_{zp_n} = \sqrt{\frac{1}{m\omega_n}}$.[12] Nonlinearities are primarily associated with the presence of an induced tension term, which is maximized for large deformations $u(x) \gg h$. Therefore, we concentrate on systems which allow large deformations, i.e., systems with $d \gg h$. We truncate the expansion to the fourth order, as in the model employed above higher-order couplings are relevant only close to the point where the beam pulls into contact with the gate plane,[11] i.e., $\max[u(y,t)] = d$. As an example, a single-layer graphene sheet with $h = 0.34$ nm, $L = 1$ $\mu$m, $S/h = 1$ $\mu$m, $E = 1$ TPa, and mass density $\rho = 1400$ kg/m$^3$ would have $\omega_s = 250$ MHz and $E_{\rm stress} = 0.01$ eV. The validity of our assumption $u \ll d$ is subject to the constraint that $\sqrt{-h\frac{\partial_d C}{E_{\rm stress}}}V_g \ll 3\sqrt{\frac{d}{h}}$ for a resonator without initial tension.[11] For the graphene sheet described above satisfying this condition with $\sqrt{-h\frac{\partial_d C}{E_{\rm stress}}}V_g = 100$ would require that $d \gg 0.38$ $\mu$m.

## III. SELF-NONLINEARITY

Let us first consider the nonlinear effects which occur when driving mode $n$ with a driving force $f_d\cos(\omega_d t)$, $\omega_d \approx \omega_n$, disregarding the coupling to the other modes, since in the absence of direct driving of the other modes these would show up only in a higher order in the nonlinear coupling constants. We also exclude the special case when two or three times the mode frequency matches one of the other mode frequencies.[13–15] Including dissipation, the equation of motion for the amplitude $x_n$ of mode $n$ is

$$\ddot{x}_n + \omega_n^2 x_n + \gamma\dot{x}_n + 3\mathcal{T}_n x_n^2 + 4\mathcal{F}_n x_n^3 = \frac{f_d}{m}\cos(\omega_d t). \quad (3)$$

Here, $x_n = x_{zp_n}\hat{x}_n$, $\omega_n = \omega_s(\Omega_n^n)_d$, $\mathcal{T}_n \equiv \frac{1}{2}\frac{\omega_s^2}{h}(\Lambda_{nn}^n)_d$, $\mathcal{F}_n \equiv \frac{1}{2}\frac{\omega_s^2}{h^2}(\Theta_{nn}^{nn})_d$, and the subscript $d$ denotes that the tensors are written in the basis which diagonalizes $[\Omega^2]$. The frequency response function can be solved from Eq. (3)[13,16]

$$|x_n|^2 = \frac{|f_d|^2/(\omega_n m)^2}{\frac{\gamma}{2}^2 + \left[(\omega_n-\omega_d) - \frac{3}{8}\frac{D}{\omega_n}|x_n|^2\right]^2}, \quad (4)$$

where $\gamma$ is the damping constant and $D = 4\mathcal{F}_n - 10(\frac{\mathcal{T}_n}{\omega_n})^2 = 2\omega_s^2/(h^2)[(\Theta_{nn}^{nn})_d - 5(\Lambda_{nn}^n)_d^2/[2(\Omega_n^n)_d^2]]$. This frequency response function is the same as one would get when considering only the fourth-order nonlinearity $\mathcal{F}_n$, i.e., a Duffing oscillator. The effect of the third-order nonlinearity $\mathcal{T}_n$ is to shift the value of the constant $D$ in the frequency response function.[16]

An example of the voltage dependence of $D$ and the response function obtained for different dc gate voltages is plotted in Fig. 2 and shows up as a crossover from $D > 0$ (hardening) to $D < 0$ (softening). The behavior of the Duffing constant depends on the total tension $T$ of the beam, which is the sum of the initial tension $T_0$ and the tension induced by the deformation $u_{\rm dc}(x)$ caused by $V_{\rm dc}$. The latter has to be calculated self-consistently from the Euler-Bernoulli equation, as discussed in Ref. 10. In what follows, we describe this behavior in terms of the dimensionless quantity $\tau = 4TL^2/(ESh^2) = h^2T/(2E_{\rm stress}L)$. In the limit $d \gg h$, it satisfies (see Appendix)

$$\tau = \tau_0 + 2\int_0^1 u_{dc}'^2 dz = \tau_0 + \frac{\tilde{V}^4}{96\tau^2}\left(1 - \frac{3\sqrt{3}}{\sqrt{\tau}} + \frac{8}{\tau}\right), \quad (5)$$

with $\tilde{V}^2 = (-h\partial_d C V_g^2)/E_{\rm stress}$. This equation is valid provided the resultant $\tau \gtrsim 1$. The tension $\tau$ exhibits a rather complicated voltage dependence, however, its behavior can be investigated in different limiting cases. A characteristic value for the voltage can be found by substituting $\tau \equiv \tau_0$ into Eq. (5) and comparing $\tau_0$ to the second term of the right-hand side of Eq. (5). This

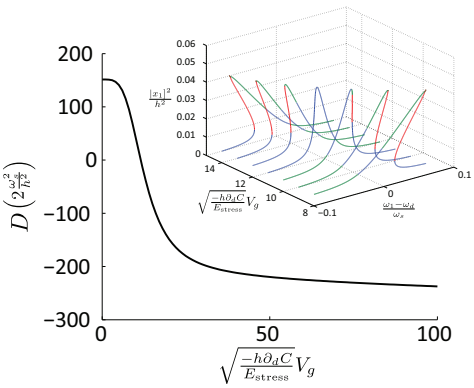


FIG. 2. (Color online) Duffing constant and frequency response function (inset) of the first mode with $\tau_0 = 0$. The Duffing constant is plotted from a numerical solution of the full Euler-Bernoulli equation obtained from (2). The response function is plotted with $\gamma^2 = 0.04\omega_s^2$ and $\frac{f^2}{\omega_1^2} = 0.002m^2\omega_s^2h^2$. Here $E_{\rm stress} = ESh^4/(8L^3)$.

yields

$$\tilde{V}^* = 96^{1/4}\frac{\tau_0^{3/4}}{\left(1-3\frac{\sqrt{3}}{\sqrt{\tau_0}}+\frac{8}{\tau_0}\right)^{1/4}}. \tag{6}$$

Thus we find that for $\tilde{V} \ll \tilde{V}^*$, the tension $\tau \approx \tau_0$, while for $\tilde{V} \gg \tilde{V}^*$, we have $\tau \approx \frac{V^{4/3}}{96^{1/3}}$. Disregarding terms coming from the electrostatic force in $\Omega_n^n$, $\Lambda_{nn}^n$, and $\Theta_{nn}^{nn}$, the general expression for the Duffing constant is (for details, see Appendix)

$$D = \frac{2\omega_s^2}{h^2}\left[(n\pi)^4 - \frac{5}{8}\frac{(n\pi)^4 f_n(\tau)^2\frac{V^4}{\tau^2}}{\frac{4I_y}{Sh^2}(n\pi^4)+\tau(n\pi)^2+f_n(\tau)^2\frac{V^4}{8\tau^2}}\right], \tag{7}$$

where $f_n(\tau) = [1-(-1)^n]n\pi\{2/(n\pi)^2 - \sqrt{3\tau}/[(n\pi)^2 + 3\tau]\}$. Note that for a symmetric dc deformation, this behavior is only valid for odd-order modes (with symmetric eigenfunctions with respect to the center of the beam). Indeed, from the expression of $f_n(\tau)$, we find that the Duffing constant is voltage independent for an even $n$. As shown in Figs. 3 and 4, at low $V_g$, $D$ starts from a positive value, $D(V_g = 0) \approx 2\omega_s^2/(h)^2(n\pi)^4$, and tends to a voltage-independent value, $2\omega_s^2/(h^2)[\frac{(n\pi)^4[(n\pi)^4-768)}{192+(n\pi)^4}]$, at large voltages. In Fig. 3, we plot the behavior of the Duffing constant for the first mode for different values of $\tau_0$. We find that $D$ changes sign for a given value of the voltage, $\tilde{V} = \tilde{V}_c$, and the effect of the initial tension is to shift the crossover voltage to higher values that can be quite well fitted to the function $\tilde{V}_c \approx \sqrt{2}\tau^{3/4} + 8$ (see Fig. 5) or

$$V_c \approx \frac{h^3}{2.4(-h\partial_d C)^{1/2}E_{\rm stress}^{1/4}}T^{3/4} + 8\frac{E_{\rm stress}^{1/2}}{-h\partial_d C}. \tag{8}$$

Contrary to the fundamental mode $n = 1$, the deformation-induced changes in the Duffing constant of higher-order modes are rather small compared to its value for $V_g = 0$ (see Fig. 4).

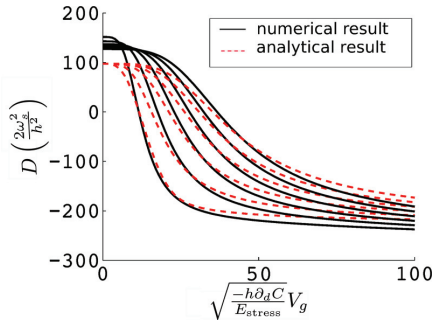


FIG. 3. (Color online) Duffing constant for the first mode with different initial tensions $\tau_0$. From left to right, the dimensionless initial tension $\tau_0$ starts from 0 and increases with the step of 10. The dashed lines are our analytic expressions and the full lines are numerical solutions of the full Euler-Bernoulli equations obtained from Eq. (2). The deviation between the two sets of curves at low $V_g$ is due to our scheme of approximating mode functions by harmonic functions. Here, $E_{\rm stress} = ESh^4/(8L^3)$.

## IV. NONLINEAR MODE COUPLING

Let us now concentrate on the nonlinear coupling between the modes.[7] Unlike in Ref. 17, where the coupling between the modes is a time-dependent linear coupling, in our system the introduction of the dc deformation leads to a radiation-pressure coupling [second term in Eq. (1)]. The regime investigated here is formally analogous to the setup encountered in optomechanical systems,[18–21] where an external driving electromagnetic field, coupled to a resonant

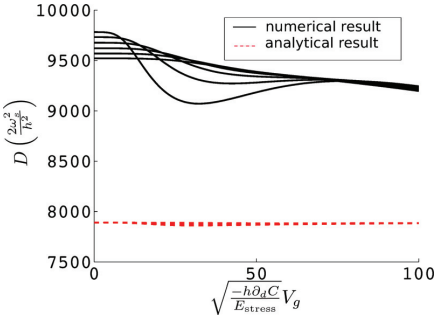


FIG. 4. (Color online) Duffing constant for the third mode with different initial tensions $\tau_0$. From left to right, the dimensionless initial tension $\tau_0$ starts from 0 and increases with the step of 10. The dashed lines are our analytic expressions and the full lines are numerical solutions of the full Euler-Bernoulli equations obtained from Eq. (2). Note that now the $V_g$ induced effect in the analytics is very small. The approximation with harmonic mode functions underestimates $\Theta_{mp}^{no}$, which is the reason for the discrepancy between the full numerical solutions and our analytic approximations. Here, $E_{\rm stress} = ESh^4/(8L^3)$.

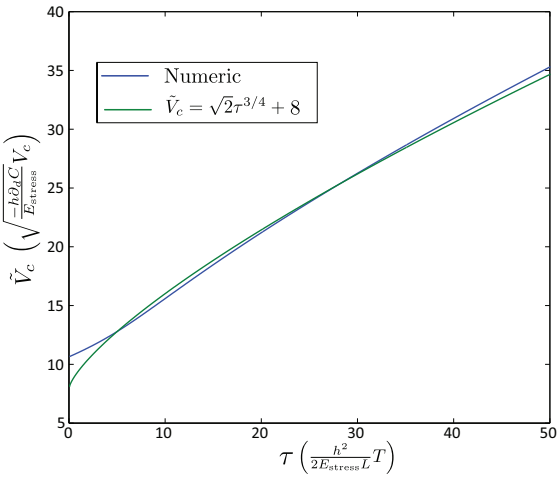


FIG. 5. (Color online) Crossover voltage $V_c$ for the sign change of the Duffing constant with respect to the initial tension $\tau_0$. Here, $E_{\rm stress} = ESh^4/(8L^3)$.

cavity, alters the characteristic response parameters of a mechanical resonator. More specifically, by aptly tuning the pump frequency, it is possible to alter the resonant frequency of the mechanical resonator (optical spring effect)[21–23] and its damping, thereby inducing cooling[20] or amplification.[21] Here we consider the case where one mechanical mode, say with eigenfrequency $\omega_m$, corresponds to the cavity mode, and another one, $\omega_n$, corresponds to the mechanical mode. We also assume that $\omega_m > 3\omega_n$. Let us discuss what happens if the system is driven with frequency $\omega_d = \omega_m - \Delta$, $\Delta \approx \pm\omega_n$, and probed around $\omega_n$.

Neglecting other modes, the Hamiltonian is of the form

$$\begin{aligned} H = {} & \omega_n \hat{a}_n^\dagger \hat{a}_n + \omega_m \hat{a}_m^\dagger a_m + T_n \hat{x}_n^3 + T_m \hat{x}_m^3 \\ & + T_{nnm} \hat{x}_n^2 \hat{x}_m + T_{nmm} \hat{x}_n \hat{x}_m^2 + F_n \hat{x}_n^4 + F_m \hat{x}_m^4 \\ & + F_{nnnm} \hat{x}_n^3 \hat{x}_m + F_{nnmm} \hat{x}_n^2 \hat{x}_m^2 + F_{nmmm} \hat{x}_n \hat{x}_m^3, \end{aligned} \quad (9)$$

where $T_{nmo}$ and $F_{nmop}$ are the sum of all the permutations of indices $n$, $m$, $o$, and $p$ of $\mathbb{T}_{nmo}$ and $\mathbb{F}_{nmop}$, respectively, and $\mathbb{T}_{nmo} = \frac{m\omega_s^2}{h} x_{zp_n} x_{zp_m} x_{zp_o} (\Lambda^n_{mo})_d$, $\mathbb{F}_{nmol} = \frac{m\omega_s^2}{h^2} x_{zp_n} x_{zp_m} x_{zp_l} x_{zp_o} (\Theta^{no}_{ml})_d$, $T_n \equiv T_{nnn}$, and $T_m \equiv T_{mmm}$. Using the input/output formalism,[24] the equations of motion for operators $\hat{a}_n$ and $\hat{a}_m$ are

$$\begin{aligned} \dot{\hat{a}}_n = {} & -i\Big[\omega_n \hat{a}_n + 4F_n x_n^3 + 3T_n x_n^2 + 4F_{nnmm}\left(\hat{a}_m^\dagger \hat{a}_m + \frac{1}{2}\right) x_n \\ & + 2T_{nmm}\left(\hat{a}_m^\dagger \hat{a}_m + \frac{1}{2}\right)\Big] - \frac{\gamma_n}{2}\hat{a}_n + \sqrt{\gamma_n}\hat{a}_n^{in}, \end{aligned} \quad (10)$$

$$\begin{aligned} \dot{\hat{a}}_m = {} & -i\big[\Delta \hat{a}_m + 12F_m \hat{a}_m (\hat{a}_m^\dagger \hat{a}_m) \\ & + 2\big(T_{mmn}\hat{x}_n + F_{nnmm}\hat{x}_n^2\big)\hat{a}_m\big] - \frac{\gamma_m}{2}\hat{a}_m + \sqrt{\gamma_m}\hat{a}_m^{in}. \end{aligned} \quad (11)$$

Here we have written operator $\alpha_m$ in a frame rotating with a frequency $\omega_d$ and neglected the fast rotating terms. We linearize (11) and (12), rewriting the operators as a sum of a static $\alpha$ and a fluctuating part $\delta a$, $\hat{a} = \alpha + \delta\hat{a}$. Keeping terms which are of the order of $(\frac{x_{zpn}}{h})^2$, we obtain $\alpha_n + \alpha_n^* \approx \frac{-4T_{nmm}|\alpha_m|^2}{\omega_n}$. Solving for $\delta\hat{a}_n$, we find the frequency response function for the input signal $\delta a_n^{in}$. It is a Lorentzian function peaked at

$$\frac{\omega_{n,\rm eff} - \omega_n}{4|\alpha_m|^2} = F_{nnmm} - 6\frac{T_n T_{nmm}}{\omega_n} \mp \frac{1}{2}\frac{T_{nmm}^2}{\omega_n} \quad (12)$$

and whose width is

$$\frac{\gamma_{n,\rm eff} - \gamma_n}{4|\alpha_m|^2} = \pm\frac{T_{nmm}^2}{\omega_m} Q_m. \quad (13)$$

Here $Q_m = \omega_m/\gamma_m$ is the quality factor of mode $m$ and we have assumed for simplicity the fully side-band resolved limit $\omega_n \gg \gamma_m$. We remark that the results are similar to those obtained in optomechanics; the only difference comes from the second term in the effective frequency, which is proportional to the self-nonlinearity. As in the case of Duffing nonlinearity, we consider the limit of $\tau \gtrsim 1$. We find that the effective frequency when driving mode $m = 3$ and probing mode $n = 1$ depends on the gate voltage as (for details, see Appendix)

$$\frac{\omega_{1,\rm eff} - \omega_1}{9\chi\pi^4} = 8 - \frac{3f_1(\tau)^2 \frac{\tilde{V}^4}{\tau^2}}{g_1(\tilde{V},\tau)} \mp \frac{3}{2}\frac{f_1(\tau)^2 \frac{\tilde{V}^4}{\tau^2}}{\sqrt{g_1(\tilde{V},\tau) g_3(\tilde{V},\tau)}}, \quad (14)$$

where $g_n(\tilde{V},\tau) = \frac{4I_y(n\pi)^4}{Sh^2} + \tau(n\pi)^2 + f_n(\tau)^2\frac{\tilde{V}^4}{8\tau^2}$ and $\chi = 4m\omega_s^2|\alpha_m|^2 x_{zp_m}^2 \frac{x_{zpn}^2}{h^2}$ describes the amplitude of the pump. The effective damping changes as

$$\frac{\gamma_{1,\rm eff} - \gamma_1}{\chi Q_3} = \pm\frac{2(3\pi)^4 f_1(\tau)^4 \frac{\tilde{V}^4}{4\tau^2}}{g_3(\tilde{V},\tau)}. \quad (15)$$

In Fig. 6, we plot the effective frequency and the effective damping when driving mode $m = 3$ and probing its effect on mode $n = 1$. We see that both for the red- and blue-detuned pumping, i.e., $\Delta = \pm\omega_1$, the frequency shift induced by pumping, $\omega_{1,\rm eff} - \omega_1$,[25] is positive at low gate voltages due to the fourth-order term $F_{1133}$ in Eq. (12), changes sign upon an increasing dc gate voltage, and tends to a voltage-independent value at large voltages. The fact that the overall frequency shift is in both cases negative—in contrast to the traditional optomechanical setup—is related to the second term in Eq. (12), which reflects the effect of the self-nonlinearity $T_n$, and which is independent of the sign of $\Delta$. This behavior applies only to the combination $n = 1$, $m = 3$. For higher-order $n$, the voltage-induced changes are small compared to the frequency shift at $V_{\rm dc} = 0$ (Fig. 8). However, choosing $n = 1$ and higher $m$ results in more complex behavior and the spring effect, $\omega_{1,\rm eff} - \omega_1$, may change sign more than once in the case of blue detuning (Fig. 7). On the other hand, the change in the effective damping (inset of Fig. 6) depends on the sign of $\Delta$. For red detuning, $\Delta = \omega_n$, $\gamma_{n,\rm eff}$ increases as the voltage is increased, whereas for blue detuning, $\gamma_{n,\rm eff}$ decreases. For a fixed amount of fluctuations coupling to mode $n$, the increase in damping leads to (side-band) cooling,[20] whereas the decreasing damping leads to heating and, when $\gamma_{\rm eff}$ becomes zero, to a parametric instability.[26] Between these regimes, the blue-detuned driving can be used for signal amplification.[21]

In conclusion, we have derived the Hamiltonian of a thin doubly clamped nanomechanical resonator taking into account

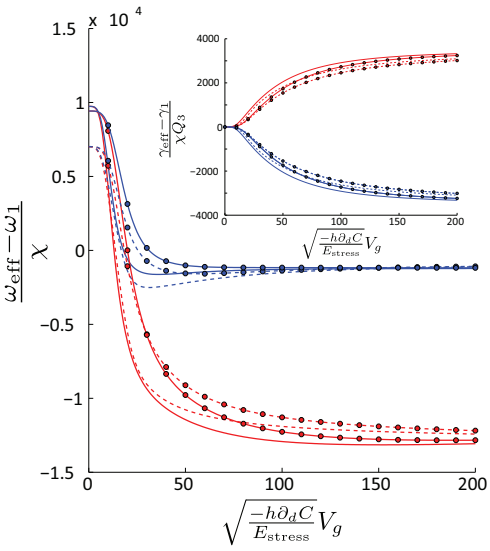


FIG. 6. (Color online) Effective frequency and damping (inset) of mode $n = 1$ when driving mode $m = 3$ with initial tension $\tau_0 = 0$ (no symbols) and $\tau = 10$ (circles) in the case of red detuning (red lines, lower) with $\Delta = \omega_1$ and in the case of blue detuning (blue lines, upper) with $\Delta = -\omega_1$. The full lines are numerical results obtained by solving the full Euler-Bernoulli equation obtained by requiring $u(x,t)$ to minimize the energy in Eq. (2), and dashed lines follow Eqs. (5), (14), and (A8). Here, $\chi = 4m\omega_s^2|\alpha_m|^2 x_{zp_m}^2 \frac{x_{zp_m}^2}{h^2}$ and $E_{\rm stress} = ESh^4/(8L^3)$.

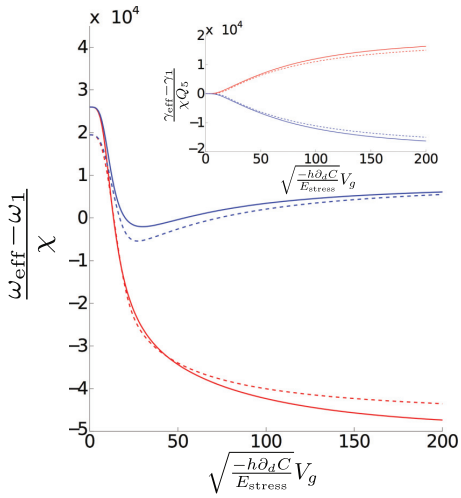


FIG. 7. (Color online) Effective frequency and damping (inset) of mode $n = 1$ when driving mode $m = 5$ and when initial tension $\tau_0 = 0$ in the case of red detuning (red lines, lower) with $\Delta = \omega_1$ and in the case of blue detuning (blue lines, upper) with $\Delta = -\omega_1$. The full lines are numerical results obtained by solving the full Euler-Bernoulli equation and the dashed lines are analytical results derived in the text.

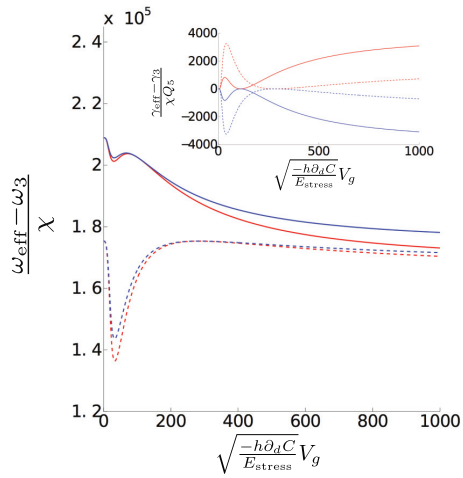


FIG. 8. (Color online) Effective frequency and damping (inset) of mode $n = 3$ when driving mode $m = 5$ and when initial tension $\tau_0 = 0$ in the case of red detuning (red lines, lower) with $\Delta = \omega_3$ and in the case of blue detuning (blue lines, upper) with $\Delta = -\omega_3$. The full lines are numerical results obtained by solving the full Euler-Bernoulli equation and dashed lines are analytical results derived in the text.

the nonlinearities between the amplitudes of the flexural modes induced by a nearby gate voltage. Besides the Duffing nonlinearity, we also find a third-order nonlinearity directly related to the dc deformation of the beam. This third-order nonlinearity adds to the Duffing nonlinearity and changes the behavior of the frequency response function. Besides the self-nonlinearity described by the Duffing behavior, we find that the different modes of the beam are nonlinearly coupled. The effective Hamiltonian of a pair of such modes resembles that of a mechanical degree of freedom coupled to a cavity, with the difference that in the current setup, the cavity is replaced by another flexural mode. Therefore, such a coupling offers the possibility of observing the motion of one mode via its effect on another mode. Such effects are the spring effect and the changing damping, and the latter can be used for side-band cooling or amplification of a given mechanical mode.

Besides the nonlinearity induced by bending described here, there may be other sources of nonlinearity in thin metallic beams, such as those related to nonlinearities in electronic properties[27] or nonlinearities induced by stretching. Our results help to identify the direct bending-induced nonlinearities and therefore facilitate the precise tuning of nanomechanical resonances.

## ACKNOWLEDGMENTS

We thank Mika Sillanpää, Sung Un Cho, and Xuefeng Song for useful discussions. This work is supported in part by the Academy of Finland Center of Excellence program, by the European Research Council (Grant No. 240362-Heattronics), and by the EU-FP7 MICROKELVIN.

## APPENDIX

### 1. Derivation of the nonlinear Hamiltonian

Expanding $u_{\rm ac}$ in Eq. (2) of the main text on an arbitrary basis $\chi_n(x)$, $u_{\rm ac} = h\sum_n y_n\chi_n$, we get the Hamiltonian of the form

$$H = \frac{p_n^2}{2m} + E_{\rm stress}\left\{[\Omega^2]^n_m y_n y^m + \Lambda^n_{mo} y_n y^m y^o + \Theta^{no}_{mp} y_n y^m y_o y^p\right\} + E_g, \tag{A1}$$

with the nonlinear coefficients

$$[\Omega^2]^n_m = \frac{\omega_0^2}{\omega_s^2}\langle\chi_n''|\chi_m''\rangle + \tau\langle\chi_n'|\chi_m'\rangle + 2\langle\chi_n'|\chi_m'\rangle\langle u_{\rm dc}'|u_{\rm dc}'\rangle + 4\langle u_{\rm dc}'|\chi_n'\rangle\langle u_{\rm dc}'|\chi_m'\rangle - \frac{V_{\rm dc}^2}{m\omega_s^2h^2}\int_0^1\frac{d^2C[d-u(x,t)]}{du_{\rm ac}^2}\langle\chi_n|\chi_m\rangle dx, \tag{A2a}$$

$$\Lambda^n_{mo} = 4\langle u_{\rm dc}'|\chi_o'\rangle\langle\chi_n'|\chi_m'\rangle - \frac{V_{\rm dc}^2}{m\omega_s^2h^2}\int_0^1\frac{d^3C[d-u(x,t)]}{du_{\rm ac}^3}\chi_n\chi_m\chi_o dx, \tag{A2b}$$

$$\Theta^{no}_{mp} = \langle\chi_n'|\chi_m'\rangle\langle\chi_o'|\chi_p'\rangle - \frac{V_{\rm dc}^2}{m\omega_s^2h^2}\int_0^1\frac{d^4C[d-u(x,t)]}{du_{\rm ac}^4}\chi_n\chi_m\chi_p\chi_o dx, \tag{A2c}$$

$$E_g = \left(2V_{\rm dc}V_{\rm ac} + V_{\rm ac}^2\right)\int_0^1 f(u_0(x))dx. \tag{A2d}$$

Here, $C[d]$ is the capacitance between the gate and the beam at the distance $d$, $\frac{1}{2}m\omega_0^2h^2 = \frac{EI}{2L^3}$ is the bending energy of a beam displaced by $h$, and $\frac{1}{2}m\omega_s^2h^2 = \frac{ESh^4}{8L^3}$ is the stress energy of the beam displaced by $h$ with respect to its equilibrium position. The coefficient $E_g$ describes the feedback of the motion of the resonator on the gate voltage and is neglected below as we assume a fixed voltage drive. Besides the voltage, the system is described by the two dimensionless parameters $\tau_0 = 4T_0L^2/(ESh^2)$ and $(\omega_0/\omega_s)^2 = 4I_y/(Sh^2)$. For a rectangular beam, which we consider in the following, $(\omega_0/\omega_s)^2 = 1/3$. Overall, our main results do not greatly depend on $\omega_0$. The thickness $h$ appears in the above expressions only because it sets the magnitude of the deformation—it scales out from the final results of observable quantities.

Writing the Hamiltonian in the basis which diagonalizes $\Omega$ and scaling $hy_n$ by the amplitude of the zero-point motion $\sqrt{1/m\omega_n}$, one arrives at Eq. (1) of the main text. We consider here specifically a doubly clamped beam. For low gate voltage $V_g$, the dc deformation $u_{\rm dc}$ is given by the Euler-Bernoulli equation in the case of a parallel plate capacitance model:

$$m\omega_0^2h\,u_{\rm dc}'''' - \left(m\omega_T^2h + 2m\omega_s^2h\int_0^1 u_{\rm dc}'^2dx\right)u_{\rm dc}'' = \frac{V_g^2}{2}\frac{\epsilon WL}{d^2}. \tag{A3}$$

The solution of this integro-differential equation is[10]

$$u_{\rm dc} = \frac{\tilde V^2}{8\tau\xi}\left\{\coth\left(\frac{\xi}{2}\right)[\cosh(\xi x)-1] - \sinh(\xi x) + \xi x - \xi x^2\right\}, \tag{A4}$$

where $\tilde V^2 = (-h\partial_d C V_g^2)/E_{\rm stress}$ and $E_{\rm stress} = m\omega_s^2h^2/2 = ESh^4/(8L^3)$. We define the total tension

$$\tau = \tau_0 + 2\int_0^1 u_{\rm dc}'^2dx \tag{A5}$$

and $\xi = \sqrt{3\tau}$. Substituting Eq. (A4) into (A5) and integrating and then disregarding exponential terms $\sim\exp(-\xi)$ yields a self-consistency equation for $\tau$, i.e., Eq. (5).

Since in the limit of large $\tau$, Eq. (A3) reduces to the wave equation, we use the harmonic wave function $\chi_n = \sqrt{2}\sin(n\pi x)$ as a basis for (A3) and get

$$[\Omega^2]^n_m = \frac{(n\pi)^4}{3} + \tau(n\pi)^2 + \frac{\tilde V^4}{8\tau^2}f_n(\tau)f_m(\tau) - \frac{\tilde V^2}{2}\frac{h}{d}, \tag{A6a}$$

$$\Lambda^n_{mo} = \sqrt{2}(n\pi)^2\frac{\tilde V^2}{2\tau}f_o(\tau)\delta^n_m - \frac{\tilde V^2}{2}\left(\frac{h}{d}\right)^2\frac{4\sqrt{2}mno[(-1)^{m+n+o}-1]}{\pi(m-n-o)(m+n-o)(m-n+o)(m+n+o)}, \tag{A6b}$$

$$\Theta^{no}_{mp} = (n\pi)^2(p\pi)^2\delta^n_m\delta^o_p - \frac{\tilde V^2}{2}\left(\frac{h}{d}\right)^3\frac{1}{2}[\delta_{n+m+o,-p} + \delta_{n+m,o+p} + \delta_{n+p,m+o} + \delta_{n+o,m+p} - \delta_{n+m+o,p} - \delta_{n+m+p,o} - \delta_{n+o+p,m} - \delta_{m+o+p,n}], \tag{A6c}$$

$$f_n(\tau) = n\pi[1-(-1)^n]\left(\frac{2}{\pi^2n^2} - \frac{\sqrt{3\tau}}{\pi^2n^2+3\tau}\right). \tag{A6d}$$

The last terms in Eqs. (A6a)–(A6c) are relevant only for low voltages in the presence of initial tension and do not greatly contribute to the physics discussed in this paper. We thus drop them out in the ensuing analytical approximations. However, in the numerical results, we use the full solutions of the Euler-Bernoulli equation to determine the eigenmodes and the coupling constants. Nevertheless, Eqs. (A6a)–(A6c) represent fair approximations in the limit of relatively strong tension.

### 2. Mode coupling

The frequency response function $f$ for the input signal $\delta a_n^{\rm in}$ solved from Eqs. (10) and (11) is

$$f = -i\sqrt{\gamma_n}\frac{\left[\Delta^2+\left(\frac{\gamma_m}{2}-i\omega\right)^2-c^2|\alpha_m|^4\right]\left[a+i\frac{\gamma_n}{2}+\omega+\omega_n\right]-2b^2|\alpha_m|^2(\Delta+c|\alpha_m|^2)}{\left[\Delta^2+\left(\frac{\gamma_m}{2}-i\omega\right)^2-c^2|\alpha_m|^4\right]\left[\left(\frac{\gamma_n}{2}-i\omega\right)^2+\omega_n^2+2a\omega_n\right]-4\omega_1 b^2|\alpha_m|^2(\Delta+c|\alpha_m|^2)}, \tag{A7}$$

with

$$\begin{aligned} a &= 12F_n(\alpha_n+\alpha_n^*)^2+6T_n(\alpha_n+\alpha_n^*)+4F_{nnmm}|\alpha_m|^2+2F_{nnmm},\\ b &= 4F_{nnmm}(\alpha_n+\alpha_n^*)+2T_{nmm},\\ c &= 12F_m. \end{aligned}$$

This frequency response function describes a Lorentzian resonance around an effective frequency $\omega_{n,\rm eff}$ with damping $\gamma_{n,\rm eff}$ described in Eqs. (12) and (13). Using the approximations leading to Eqs. (A2), we find the effective frequency

$$\frac{\omega_{n,\rm eff}-\omega_n}{\chi} = n^2m^2\pi^4\left\{8-\frac{3f_n(\tau)^2\frac{\tilde V^4}{\tau^2}}{\frac{4I_y(n\pi)^4}{Sh^2}+\tau(n\pi)^2+f_n(\tau)^2\frac{\tilde V^4}{8\tau^2}} \mp \frac{m^2}{4n^2}\frac{f_n(\tau)^2\frac{\tilde V^4}{\tau^2}}{\sqrt{\left[\frac{4I_y(n\pi)^4}{Sh^2}+\tau(n\pi)^2+f_n(\tau)^2\frac{\tilde V^4}{8\tau^2}\right]\left[\frac{4I_y(m\pi)^4}{Sh^2}+\tau(m\pi)^2+f_m(\tau)^2\frac{\tilde V^4}{8\tau^2}\right]}}\right\}$$

and effective damping

$$\frac{\gamma_{n,\rm eff}-\gamma_n}{\chi Q_m} = \pm\frac{2(m\pi)^4f_n(\tau)^2\frac{\tilde V^4}{4\tau^2}}{\frac{4I_y(m\pi)^4}{Sh^2}+\tau(m\pi)^2+f_m(\tau)^2\frac{\tilde V^4}{8\tau^2}}. \tag{A8}$$

Here, $\chi = 4m\omega_s^2|\alpha_m|^2x_{zp_m}^2\frac{x_{zp_n}^2}{fh^2}$ describes the amplitude of the pump.

In Fig. 6 of the main text, we plot the effective frequency and the effective damping when driving mode $m=3$ and probing its effect on mode $n=1$. Considering only odd modes $n$, we see that for red-detuned pumping with $\Delta=\omega_n$, the frequency shift induced by pumping is positive at low gate voltages, $\omega_{n,\rm eff}(V_g=0)-\omega_n=(n\pi)^2(m\pi)^2\chi$, changes sign with increasing dc gate voltage, and tends to a voltage-independent value at large voltages,

$$\omega_{n,\rm eff}-\omega_n \overset{\tilde V\gg\tau_0,1}{\longrightarrow} \chi(nm)^2\pi^4\left\{8-\frac{4608/(n\pi)^2}{(n\pi)^2+192/(n\pi^2)}-\frac{m^2}{n^2}\frac{384/(n\pi)^2}{\sqrt{[(n\pi)^2+192/(n\pi^2)][(m\pi)^2+192/(m\pi^2)]}}\right\}. \tag{A9}$$

On the other hand, the effective damping increases with an increasing gate voltage until it reaches a voltage-independent value,

$$\frac{\gamma_{n,\rm eff}-\gamma}{\chi Q_m} = \frac{m^6}{n^4}\frac{768\pi^4}{\pi^4m^4+192}. \tag{A10}$$

For blue-detuned driving, when $\Delta=-\omega_n$, the optical spring effect ($\omega_{n,\rm eff}-\omega$) increases until it saturates at large voltages to the value

$$\omega_{n,\rm eff}-\omega_n \overset{\tilde V\gg\tau_0,1}{\longrightarrow} \chi(nm)^2\pi^4\left\{8-\frac{4608/(n\pi)^2}{(n\pi)^2+192/(n\pi^2)}+\frac{m^2}{n^2}\frac{384/(n\pi)^2}{\sqrt{[(n\pi)^2+192/(n\pi^2)][(m\pi)^2+192/(m\pi^2)]}}\right\}, \tag{A11}$$

while the damping decreases until it reaches the value

$$\frac{\gamma_{n,\rm eff}-\gamma}{\chi Q_m} = -\frac{m^6}{n^4}\frac{768\pi^4}{\pi^4m^4+192}. \tag{A12}$$

These predictions are compared to the full numerical solutions obtained from the Hamiltonian given by Eq. (2) in Figs. 6–8.

*raphael.khan@aalto.fi

[1] K. Jensen, K. Kim, and A. Zettl, Nature Nanotech. **3**, 533 (2008).
[2] J. Chaste, A. Eichler, J. Moser, G. Ceballos, R. Rurali, and A. Bachtold, Nature Nanotech. **7**, 301 (2012).
[3] E. Gavartin, P. Verlot, and T. J. Kippenberg, Nature Nanotech. **7**, 509 (2012).
[4] J. S. Bunch, A. M. v. d. Zande, S. S. Verbridge, I. W. Frank, D. M. Tanenbaum, J. M. Parpia, H. G. Craighead, and P. L. McEuen, Science **315**, 490 (2007).
[5] A. D. O'Connell, M. Hofheinz, M. Ansmann, R. C. Bialczak, M. Lenander, E. Lucero, M. Neeley, D. Sank, H. Wang, M. Weides, J. Wenner, J. M. Martinis, and A. N. Cleland, Nature (London) **464**, 697 (2010).
[6] A. K. Hüttel, G. A. Steele, B. Witkamp, M. Poot, L. P. Kouwenhoven, and H. S. J. van der Zant, Nano Lett. **9**, 2547 (2009).
[7] H. J. R. Westra, M. Poot, H. S. J. van der Zant, and W. J. Venstra, Phys. Rev. Lett. **105**, 117205 (2010).
[8] K. J. Lulla, R. B. Cousins, A. Venkatesan, M. J. Patton, A. D. Armour, C. J. Mellor, and J. R. Owers-Bradley, New J. Phys. **14**, 113040 (2012).
[9] L. D. Landau, E. M. Lifshitz, A. M. Kosevich, and L. P. Pitaevski, *Theory of Elasticity* (Elsevier, New York. 1986).
[10] S. Sapmaz, Y. M. Blanter, L. Gurevich, and H. S. J. van der Zant, Phys. Rev. B **67**, 235414 (2003).
[11] M. A. Sillanpää, R. Khan, T. T. Heikkilä, and P. J. Hakonen, Phys. Rev. B **84**, 195433 (2011).
[12] Even though in the following we concentrate on driving amplitudes containing many photons, and therefore deal with essentially classical nonlinearities, quantum effects related with zero-point motion could also be discussed with the Hamiltonian we derive.
[13] A. H. Nayfeh and D. T. Mook, *Nonlinear Oscillations* (Wiley, New York, 2008).
[14] D. Antonio, D. H. Zanette, and D. López, Nature Commun. **3**, 806 (2012).
[15] A. Eichler, M. del Álamo Ruiz, J. A. Plaza, and A. Bachtold, Phys. Rev. Lett. **109**, 025503 (2012).
[16] I. Kozinsky, H. W. C. Postma, I. Bargatin, and M. L. Roukes, Appl. Phys. Lett. **88**, 253101 (2006).
[17] I. Mahboob, K. Nishiguchi, H. Okamoto, and H. Yamaguchi, Nature Phys. **8**, 387 (2012).
[18] F. Marquardt, J. P. Chen, A. A. Clerk, and S. M. Girvin, Phys. Rev. Lett. **99**, 093902 (2007).
[19] C. Genes, D. Vitali, P. Tombesi, S. Gigan, and M. Aspelmeyer, Phys. Rev. A **77**, 033804 (2008).
[20] J. D. Teufel, T. Donner, D. Li, J. W. Harlow, M. S. Allman, K. Cicak, A. J. Sirois, J. D. Whittaker, K. W. Lehnert, and R. W. Simmonds, Nature (London) **475**, 359 (2011).
[21] F. Massel, T. T. Heikkilä, J. Pirkkalainen, S. U. Cho, H. Saloniemi, P. J. Hakonen, and M. A. Sillanpää, Nature (London) **480**, 351 (2011).
[22] J. D. Teufel, J. W. Harlow, C. A. Regal, and K. W. Lehnert, Phys. Rev. Lett. **101**, 197203 (2008).
[23] T. Rocheleau, T. Ndukum, C. Macklin, J. B. Hertzberg, A. A. Clerk, and K. C. Schwab, Nature (London) **463**, 72 (2009).
[24] C. W. Gardiner and M. J. Collett, Phys. Rev. A **31**, 3761 (1985).
[25] Note that tuning the gate voltage also changes the bare frequencies $\omega_n$. What we consider here is the additional frequency shift due to the driving of mode $m \neq n$.
[26] T. J. Kippenberg, H. Rokhsari, T. Carmon, A. Scherer, and K. J. Vahala, Phys. Rev. Lett. **95**, 033901 (2005).
[27] A. Castellanos-Gomez, H. B. Meerwaldt, W. J. Venstra, H. S. J. van der Zant, and G. A. Steele, Phys. Rev. B **86**, 041402 (2012).